

Electronic Transitions in Near-Equiatomic Vanadium-Ruthenium Alloys

C. W. Chu, * E. Bucher, A. S. Cooper, and J. P. Maita
Bell Telephone Laboratories, Murray Hill, New Jersey 07974

(Received 5 January 1971)

The electrical resistivity, the magnetic susceptibility, and the Knight shift of V^{51} have been studied as a function of temperature in near-equiatomic V-Ru alloys. Electronic transitions were observed as evidenced by the following anomalies: Over a narrow temperature range, the resistivity increases sharply, the susceptibility decreases rapidly, and the Knight shift increases during cooling. At the same time, a tetragonal crystallographic distortion occurs, as found by Marezio *et al.* The low-temperature specific heat and the superconducting transition temperature were found to vary drastically over the concentration region of interest in agreement with the results of previous work. These changes in electronic properties can be consistently interpreted as arising from a substantial reduction in the Fermi-surface area and of the effective number of carriers associated with the tetragonal distortion. This further suggests that the tetragonal phase is stabilized by the reduction of the electronic free energy.

I. INTRODUCTION

The electronic properties of transition metals and alloys have been extensively studied. In general the Sommerfeld coefficient of the specific heat¹ (γ) peaks sharply at $\bar{z} \approx 4.7$ and ≈ 6.4 , where \bar{z} denotes the electron-per-atom ratio. A simple rigid-band model² constructed from the γ measurements can account quite well for the magnetic susceptibility (χ_m) and the nuclear magnetic resonance (NMR) results. However, in some alloy systems, γ decreases rapidly (almost discontinuously), and the superconducting transition temperature (T_c) drops to below 0.4 K before γ reaches the maximum at $\bar{z} \approx 6.4$. The V-Ru alloy series is one such series, and it has been investigated carefully by various authors. Raub and Fritzsche³ have investigated the phase diagram of the V-Ru system between 1100 and 1600 °C. They found that V and Ru form alloys progressing through body-centered cubic (bcc), CsCl (*B2*, cubic), tetragonal CsCl (tetr.*B2*), and hexagonal closed packed (hcp) structures as the concentration of Ru increases. Based on this phase diagram, Flükiger *et al.*⁴ concluded that the abrupt decrease of γ as a function of composition was a direct consequence of a Jahn-Teller-type deformation⁵ when the crystal structure changes from *B2* to tetr.*B2*. Bernasson *et al.*⁶ then observed that the Knight shift of V^{51} (K_V) and χ_m of the whole V-Ru alloy series were temperature independent and both had a break across the *B2*-tetr.*B2* phase boundary. These later findings seem to imply that the structure boundary is stable against temperature and is in agreement with the conclusion of Flükiger *et al.*

In contrast to the results of Bernasson *et al.* we observed the following: The *B2* phase of near-equiatomic V-Ru alloys is unstable against temperature variation. In samples of this crystal structure, we saw an electronic transition as evidenced

by a rapid rise in resistivity (ρ), a rapid decrease in χ_m , and an increase of K_V (in $V_{0.51}Ru_{0.49}$) over a narrow temperature range during cooling. The critical temperature (T_h) of the transition depends sensitively on the composition. At the same temperatures Marezio *et al.*⁷ found that the anomalies in the electronic properties are accompanied by a tetragonal distortion of the structure. These results lead us to the suggestion that there exists in the near-equiatomic V-Ru alloys an electronic transition associated with a reduction in the effective number of d electrons, and that the rapid drops in γ and T_c are a direct consequence of this transition. The qualitative effects on electronic properties, such as ρ , γ , and χ_m , at this transition are similar to those observed for the antiferromagnetic transition in Cr⁸ and its alloys.⁹ Clearly, since the NMR of V^{51} can be observed below T_h , this transition is not magnetic in origin. We shall compare and contrast the transition described here to the antiferromagnetic transition observed in Cr and its alloys.

II. EXPERIMENTS AND RESULTS

Vanadium-ruthenium alloys with Ru concentration (C) between 45 and 56 at. % were prepared. Appropriate amounts of V (Gallard-Schlesinger 99.9-wt% purity) and Ru (Engelhard 99.95-wt% purity) were arc melted on a water-cooled copper hearth in an argon atmosphere. To promote homogeneity, each sample was turned and remelted at least seven times. A sample button of ~ 0.3 in. diam by ~ 0.5 in. long was cut into halves along the long axis. Fluorescent x-ray spectroscopy revealed no macroscopic composition gradients across the cut surface. Two of the samples were annealed in vacuum at 1000 °C for a week in a quartz tube. This did not generate any noticeable change in ρ , χ_m , or T_h . Therefore all measurements except the

TABLE I. Room-temperature x-ray and other data for samples investigated.

Sample	Crystal structure	T_c (K)	T_h (K)	λ	Θ_D (K)
$V_{0.55}Ru_{0.45}$	$B2(s)^a$	4.0	< 4		413 ^b
$V_{0.54}Ru_{0.46}$	$B2(s)$	5.0	56	0.57(9)	429
$V_{0.53}Ru_{0.47}$	$B2(s)$	2.3	135	0.48(2)	456
$V_{0.52}Ru_{0.48}$	$B2(s)$	< 1	210		
$V_{0.51}Ru_{0.49}$	$B2(s)$	< 0.4	290		
$V_{0.50}Ru_{0.50}$	$B2(m) + tetr. B2(s)^c$	< 0.4	365	< 0.38(8)	420 ^b
$V_{0.49}Ru_{0.51}$	$B2(w) + tetr. B2(s) + ?(w)^d$	< 1	425	< 0.42(6)	427 ^b
$V_{0.48}Ru_{0.52}$	$B2(vw)^e + Tetr. B2(s) + hcp(m)$	3.2	480		
$V_{0.46}Ru_{0.54}$	$B2(w) + tetr. B2(ms) + hcp(m)$	3.5	600		

^as: strong.^bAfter Ref. 1.^cm: medium.^dw: weak.^evw: very weak.

x-ray study were done on the as-cast samples.

Each sample was examined by powder x-ray diffraction at room temperature in the as-ground (strained) and annealed state. The structures of the annealed samples, in general, agree with those of Raub and Fritzsche.³ In the composition range in which we are interested, only the $B2$ phase is present for $45 \leq C \leq 49$; the $tetr. B2$ phase also occurs for $C \geq 50$; and the hcp phase appears in addition to $B2$ and $tetr. B2$ for $C \geq 52$. These results are summarized in Table I. All strained powder samples show bcc structure for $46 \leq C \leq 51$ and bcc + $tetr. B2$ structure for $C \geq 51$ (even with some hcp phase for $C \geq 52$). This indicates that the crystal structure for samples near the $B2$ - $tetr. B2$ boundary is extremely sensitive to strain introduced through grinding. Annealing in vacuum at $\sim 950^\circ C$ for ~ 36 h will restore the ordered structure, $B2$ or $tetr. B2$. In order to identify the crystal structure of the bulk material with that of the annealed powder, we measured χ_m as a function of temperature of a sample in the following different states: as cast, strained powder, and annealed powder. It was found that $\chi_m(T)$ is the same for the as-cast sample as for the annealed powder, while χ_m is reduced considerably at $T > T_h$ and enhanced slightly at $T < T_h$. Hence we conclude that the crystal structures for annealed powder samples given in Table I represent those for the bulk samples on which ρ , χ_m , γ , K_V , and T_c were measured.

Sample bars of cross section ~ 0.03 cm² and length ~ 1.5 cm were cut from the as-cast button with a carborundum wheel. Platinum leads were spot welded onto them. A standard four-lead dc technique was employed to determine ρ from 4 to 410 K. For samples of $46 \leq C \leq 51$, where only the $B2$ phase is present at $T > T_h$, when T is lowered ρ decreases initially as for an ordinary metal, then rises sharply, passes a broad maximum, and finally drops slightly. No normal hysteresis > 0.5 K was detected. The results, normalized to resistivity at 405 K, plotted against temperature are shown in Fig. 1.

We define the critical temperature of the elec-

tronic transition as the temperature where ρ is minimum and χ_m is maximum (as will be discussed in Sec. III). T_h varies from 56 to 600 K as C increases from 46 to 56, as shown in Fig. 2. For $C = 45$ no sudden increase of ρ occurs before the sample becomes superconducting at 4 K. When $C > 51$, where the hcp phase is also present, T_h lies beyond the temperature range of our resistivity probe, the ρ increases become relatively smaller and more widely drawn. It is also clear from Fig. 1 that the reduced resistivities of different concentrations seem to vary in a similar way with temperature, independent of C , provided $T > T_h$. This allows us to estimate the percentage change in ρ due to the transition by evaluating the quantity $\Delta\rho/\rho_{20}$ at 20 K. $\Delta\rho$ is defined as $\rho_{20} - \rho_0$, where ρ_0 is the extrapolated value of ρ at 20 K as if there were no such transition present. $\Delta\rho/\rho_{20}$ increases rapidly and then drops off at $C \geq 50$ as shown in Fig. 3.

The χ_m was determined by a pendulum magnetometer from 1.4 to 400 K. For samples of $C > 51$, measurements were kindly extended to 700 K by Menth using a Cahn balance. In Fig. 4 the temperature variation of χ_m for different samples is

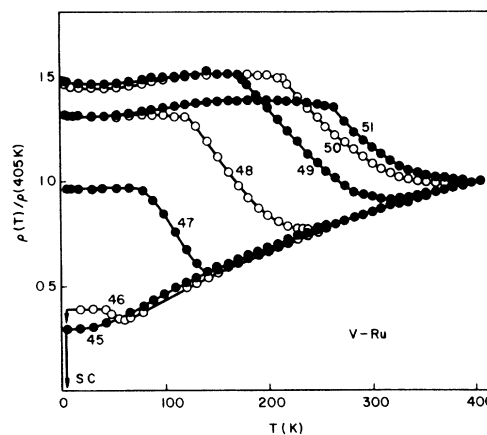


FIG. 1. Reduced electrical resistivity vs temperature. The number associated with each curve denotes the Ru concentration in at. %.

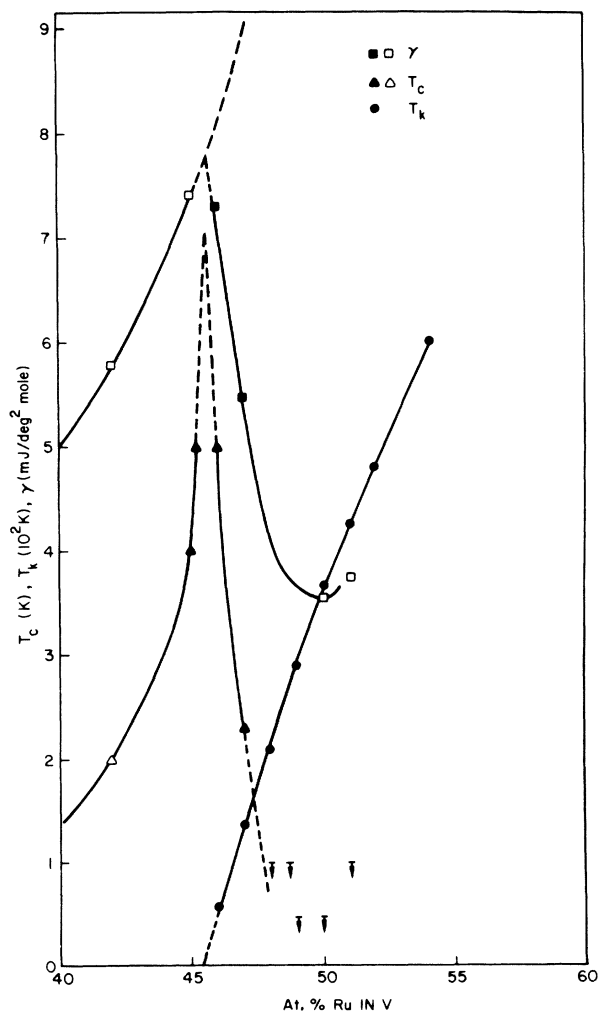


FIG. 2. Electronic transition temperature T_h , the superconducting temperature T_c , and the coefficient of electronic specific heat γ vs Ru concentration. The open symbols are taken from Ref. 4.

given. Generally χ_m increases slowly and linearly with almost a constant slope for $T > T_h$ (except for $C = 50$, where χ_m is temperature independent), reaches a maximum at $T = T_h$, decreases rapidly over the same temperature range, where ρ exhibits a steep rise, and finally flattens out. There is no thermal hysteresis to within 0.5 K observed. The fast rise at lower temperature can be accounted for by the presence of parasitic magnetic impurities, e. g., ~ 350 -ppm Fe. No spontaneous magnetic moment was found.

To demonstrate how χ_m is affected by the transition, we have plotted in Fig. 5 the maximum susceptibility $\chi_{\max}(T = T_h)$ and the minimum susceptibility χ_{\min} for different concentrations. Since at temperatures below the transition χ_m changes only slightly with T , we took χ_m at 77 or 40 K for our

χ_{\min} as is appropriate. The χ_{\max} is almost a constant when $46 \lesssim C \lesssim 50$, and then decreases drastically when $C > 50$, whereas χ_{\min} decreases sharply with $C \lesssim 50$ but only slowly with $C > 50$. The χ_{\max} and χ_{\min} can be extrapolated to cross at both ends with $C_h \approx 45.5$ and > 60 . This implies that alloys with $C < 45.5$ will no longer have an electronic transition above 0 K. At the high- C end, the crossing of χ_{\max} and χ_{\min} is misleading because of the presence of hcp phase. For nonmagnetic transition metals, the major contributions to χ_m are the spin part (χ_{spin}) and the van Vleck part (χ^{VV}). Hence

$$\Delta\chi/\chi_{\max} - \chi^{\text{VV}} \approx \chi_{\max} - \chi_{\min}/\chi_{\max} - \chi^{\text{VV}} \approx \Delta\chi_{\text{spin}}/\chi_{\text{spin}}$$

gives the relative change in electronic properties due to the transition. The χ^{VV} is obtained by making use of γ and χ_m , neglecting the Landau-Peierls term and the core contribution. It behaves in a way similar to $\Delta\rho/\rho_{20}$ as shown in Fig. 3 where it is plotted as a function of C .

Low-temperature specific-heat measurements were made on two samples with $C = 46$ and 47 using the heat-pulse technique.¹⁰ We obtained $\gamma = 7.33$ mJ/deg² mole, $\Theta_D = 429$ K for $V_{0.54}\text{Ru}_{0.46}$ and $\gamma = 5.9$

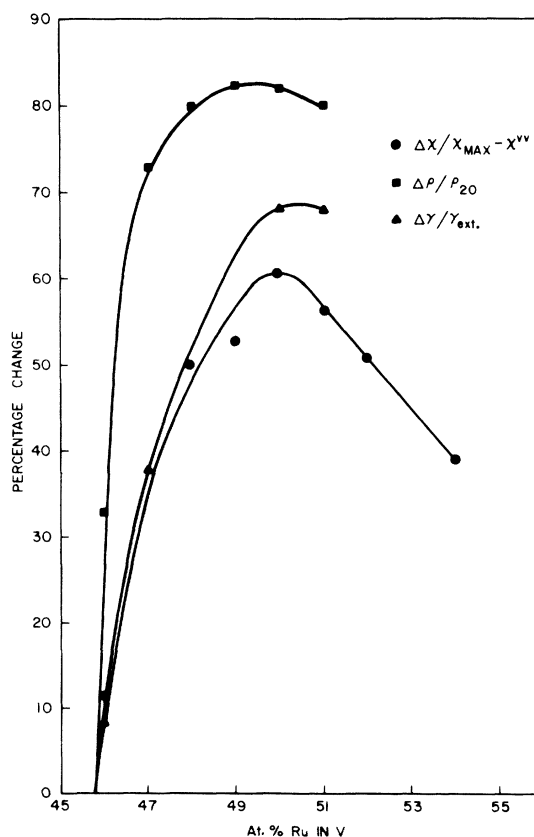


FIG. 3. Fractional change in susceptibility, resistivity, and coefficient of electronic specific heat due to the electronic transition vs Ru concentration.

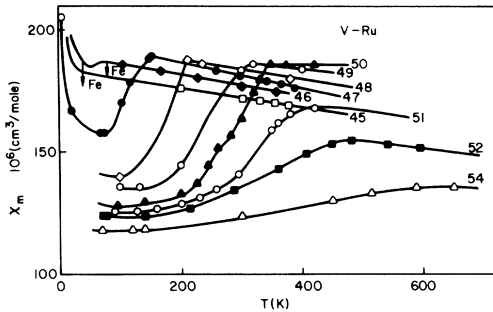


FIG. 4. Temperature variation of the susceptibility. The number associated with each curve represents the Ru concentration.

mJ/deg² mole, $\Theta_D = 456$ K for $V_{0.53}Ru_{0.47}$. Together with the γ data of other workers,¹ we find (Fig. 2) that γ decreases very rapidly but continuously with C in this region, and it rises sharply as C approaches ~ 45.5 from both sides. The specific heat of $V_{0.54}Ru_{0.46}$ which has $T_h = 56$ K was examined up to 57 K, the limit of the thermometer of our apparatus. With an accuracy of $\sim 3\%$ at this limiting temperature, we did not observe any detectable anomaly. Assuming that the sharp drop in γ for $46 < C < 51$ is caused by the transition, we estimated the percentage change of γ by calculating

$$\Delta\gamma/\gamma_{\text{ext}} \equiv \gamma_{\text{ext}} - \gamma/\gamma_{\text{ext}},$$

where γ_{ext} is the value for certain C extrapolated from $C \lesssim 45$. They are shown in Fig. 3 as a function of C and vary similarly to $\Delta\rho/\rho_{20}$ and $\Delta\chi/\chi_{\text{max}} - \chi^{\text{V}}$.

The superconductivity was detected by an ac inductance technique. For those compositions already studied by others,⁴ our results are in excellent agreement. The variation of T_c with C is plotted in Fig. 2. Similar to γ , T_c rises steeply with C approaching ~ 45.5 from both sides. No superconductivity above 0.4 K was found for C between 48 and 51. The reappearance of superconductivity at ~ 3.2 K for $C > 51$ coincides with the presence of the hcp phase in the sample. This implies that tetr. B2 phase with $C \geq 48$ is not superconducting. Preliminary measurement of K_V was made on the unstrained 170-mesh powder of $V_{0.51}Ru_{0.49}$. In contrast to the previous findings that K_V was temperature independent,⁴ we found that $K_V = +0.37\%$ at 300 K and $+0.49\%$ at 77 K in that sample.

III. DISCUSSION

In this discussion we shall restrict ourselves to consideration of samples containing $\leq 51\%$ Ru because of complications due to the occurrence of the hcp phase in samples of higher concentration. It is interesting that a change in electronic properties greater than 50% is associated with only a 6% tetrag-

onal distortion. Furthermore, for $V_{0.54}Ru_{0.46}$, although $\Delta\chi/\chi_{\text{max}} - \chi^{\text{V}} = 11\%$, no noticeable lattice-specific-heat anomaly at the transition was detected. This suggests that the transition is primarily electronic in nature. One thus can ascribe the anomalies in ρ , χ_m , γ , T_c , and K_V to such an electronic transition, arising from a change in the electron energy spectrum.

Assuming that there is a substantial removal of electrons at the Fermi surface accompanying the electronic transition, we can qualitatively explain this anomalous behavior. Following the results of our preliminary study of K_V , it can be seen that these removed electrons are of d character. As is clear from Figs. 1 and 4, ρ undergoes a steep rise while χ_m experiences a sudden drop over the same temperature region when the sample is cooled through T_h . The change in χ_m associated with the transition arises mainly from the change in the spin part of χ_m . Therefore from now on we are only concerned with χ_{spin} . Since ρ is inversely proportional to the number of conduction electrons n , and χ_{spin} to the density of state $N(\epsilon_F)$ on the Fermi surface ($\propto n^{1/3}$), the reduction of n thus leads to an increase in ρ and a decrease in χ_{spin} . The values of γ ($\propto N$) were determined from specific-heat measurements at low temperature, i. e., at $T < T_h$. Hence γ so obtained is suppressed for samples exhibiting an electronic transition (as shown in Fig. 2). Values of $\Delta\rho/\rho_{20}$, $\Delta\chi_{\text{spin}}/\chi_{\text{spin}}$, and $\Delta\gamma/\gamma_{\text{ext}}$ can then be taken as a measure of the fractional change of n , $\Delta n/n$, due to the transition. They are found to vary in step with the variation of C , as is evident from Fig. 3. The extrapolation of $\Delta\rho/\rho_{20}$, $\Delta\chi_{\text{spin}}/\chi_{\text{spin}}$, $\Delta\gamma/\gamma_{\text{ext}}$, and T_h back to zero gives a critical concentration, $C_h \approx 45.5$, i. e., no cubic to tetragonal distortion exists in V-Ru alloys with $C \lesssim 45.5$. Figure 2 shows that T_h continues to rise in contrast to the tapering

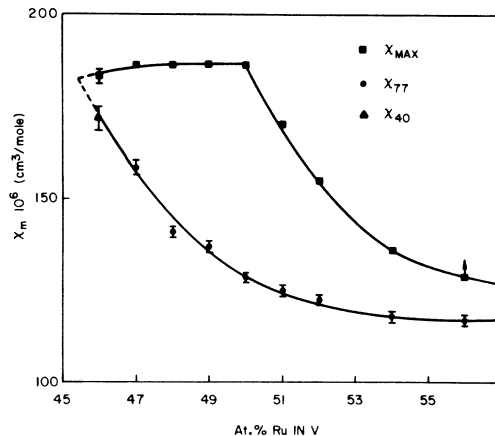


FIG. 5. Maximum and minimum susceptibilities before and after the electronic transition vs concentration.

off of $\Delta\rho/\rho_{20}$, $\Delta\chi_{\text{spin}}/\chi_{\text{spin}}$, and $\Delta\gamma/\gamma_{\text{ext}}$ for $C > 50$. In view of the different natures of these measurements, this can be understood in terms of the partial presence of the hcp phase in which no electronic transition takes place.

The low-temperature x-ray diffraction studies by Marezio *et al.*⁷ showed that a first-order cubic-to-tetragonal transition in ordered near-equiatomic V-Ru alloys takes place over a temperature interval commensurate with the observed anomalies of the present study. The transition was observed to involve a volume expansion independent of composition and temperature between 300 and 110 K. As a result, one would expect $\Delta n/n$ to be independent of C and to drop to zero very rapidly as C approaches C_h . In view of the C dependence of T_h (see Fig. 2), it is not surprising to see that this is not the exact situation observed, since there may exist in the samples a semimicroscopic distribution of C . This is further demonstrated by the broad transition, the simultaneous appearance of the *B2* and the *tetr.B2* phases at temperatures within the transition, and the fact that the T variation of the intensity of the x-ray diffraction lines characteristic of the *B2* phase has the same shape as $\chi_m(T)$.⁷ However, the present study suggests that the *tetr.B2* phase is stabilized by the reduction of the free energy associated with the electrons removed.

From the specific-heat measurements of $V_{0.54}\text{Ru}_{0.46}$ with $T_h = 56$ K, we found that at 56 K the total entropy of the sample was $S_t \approx 0.8$ cal/deg mole and the electronic part

$$S_e = \int_0^{56} \gamma T (dT/T) = 0.09 \text{ cal/deg mole.}$$

This means that at T_h only $\sim 11\%$ of the total entropy is associated with the electrons. Because the electron transition removes Δn electrons from the conduction band, we are able to estimate the accompanying fractional change in S_e by using the value of $\Delta n/n$. As was mentioned already, values of $\Delta\rho/\rho_{20}$, $\Delta\chi_{\text{spin}}/\chi_{\text{spin}}$, or $\gamma/\gamma_{\text{ext}}$ could be taken as a measure of $\Delta n/n$. We took $\Delta n/n = \Delta\chi_{\text{spin}}/\chi_{\text{spin}}$ since this quantity is considered more reliable than the others because it does not involve any extrapolation. $\Delta S_e/S_e$ so obtained is $\sim 1\%$ which is smaller than the uncertainty of our specific-heat measurement at 56 K. This is in agreement with our failure to observe any anomaly in specific heat through the electronic transition of $V_{0.54}\text{Ru}_{0.46}$.

The results of the preliminary study on K_V of $V_{0.51}\text{Ru}_{0.49}$ (with an electronic transition between 160 and 300 K) at 300 and 77 K reveal that the effective internal field at a V site is stronger at low temperature. Clogston and Jaccarino¹¹ have proposed the following modified model to interpret the Knight-shift data of the transition-metal compounds: Knight shift in transition-metal compounds is considered to arise from (i) the contact hyperfine in-

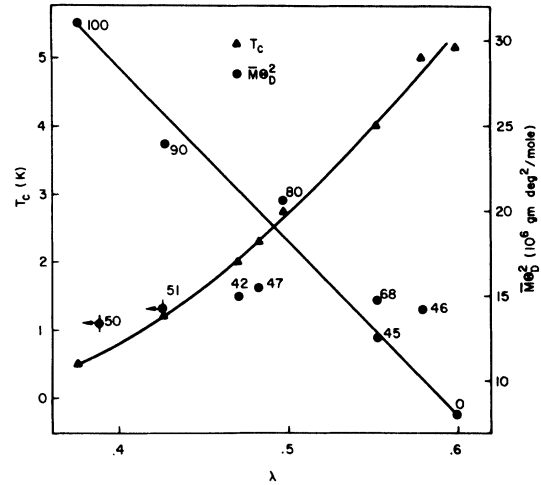


FIG. 6. Superconducting transition temperature and the stiffness of the samples vs the electron-phonon coupling constant. The number represents the Ru concentration and the bar represents the upper bound of λ .

teraction between the nuclear magnetic moments and the field due to the effective spins of the conduction electrons, minus (ii) exchange polarization of the inner-core s electrons by the d electrons. One therefore writes

$$K_V(T) = a\chi_s + b\chi_{\text{orb}} - c\chi_d(T),$$

$$\chi_m(T) = \chi_s + \chi_{\text{orb}} + \chi_d(T),$$

where χ_s and χ_d are the contributions of the electrons in the s and d bands, and χ_{orb} is the orbital part. Following this model, one can attribute the increase of K_V in the *tetr.B2* phase to the decrease of χ_d in this phase. But the coupling constant c here is an order of magnitude larger than in other compounds.¹² This is not surprising, since one generally expects the exchange polarization to be different in different electron environment. From the above considerations, we conclude that the electrons removed from the conduction band through the electronic transition are predominantly d like.

Regarding the temperature variation of χ_{spin} , the following features were observed: (a) $d\chi_{\text{spin}}/dT \approx -8 \cdot 10^{-8}$ cm³/mole deg for $T \geq T_h$ and $C \neq 50$; (b) $d\chi_{\text{spin}}/dT = 0$ for $T \geq T_h$ and $C = 50$; (c) $\chi_{\text{max}} \approx 186 \times 10^{-6}$ cm³/mole for $T = T_h$ and $C \leq 50$. Applying these boundary conditions to the expression for the spin paramagnetic susceptibility¹³

$$\chi_{\text{spin}} = \chi_0 \left[1 + \frac{\pi^2}{6} \left(\frac{\partial^2 \ln N}{\partial \epsilon^2} \right) k^2 T^2 \right]$$

we found the density of states N to be too complex a function of concentration (or energy ϵ) to enable us to gain any simple physical insight. However, it does indicate that there seems to exist a critical

value of χ_m , $\sim \chi_{\max}$, or better N , for lattice instability to occur.

We will next consider the variation of the superconducting transition temperature T_c near the equiatomic composition. According to McMillan's theory¹⁴ for strong coupling superconductors, the electron-phonon coupling constant λ is related to the Debye temperature Θ_D , the Coulomb interaction μ^* , and T_c by the following expression:

$$\lambda = \frac{1.04 + \mu^* \ln(\Theta_D/1.45T_c)}{(1 - 0.62\mu^*) \ln(\Theta_D/1.45T_c) - 1.04}$$

The λ is governed by the phonon factor $M \langle \omega^2 \rangle$ only where M is the averaged ionic mass and $\langle \omega^2 \rangle$ is the average of the square of the phonon frequencies. We have calculated λ for the superconducting alloys of the V-Ru system by using McMillan's formula and taking $\mu^* = 0.13$.¹⁴ The T_c of the single-phase sample is an increasing function of λ irrespective of the crystal structure as shown in Fig. 6. The lack of phonon-spectrum data of this system prevents us from evaluating $\langle \omega^2 \rangle$. However it is known that Θ_D^2 is a good qualitative measure of $\langle \omega^2 \rangle$. In Fig. 6 we also plotted λ against $M\Theta_D^2$, the lattice stiffness, as the theory predicts. We have also estimated the upper bound λ for the two nonsuperconducting samples, $V_{0.50}Ru_{0.50}$ and $V_{0.49}Ru_{0.51}$, by using their upper limit T_c , and they are shown in the same figure. The small stiffness $M\Theta_D^2$ and the small λ make them fall far to the left of the λ vs $M\Theta_D^2$ line for the V-Ru system. This seems to suggest that the large suppression of T_c is due to more than the loss of d electrons, or of N_d (empirically, the higher the N , the lower the stiffness). The reason is not clear. This picture may be applicable to alloy systems which have similar anomalous behavior in γ and T_c . One of the most promising systems will be Ta-Ru alloys. Study on this system and others is under way.

As we have seen, the changes in ρ , χ_m , and K_V can be readily accounted for by assuming that a large reduction in the number of d electrons at the Fermi surface accompanies the change from cubic to tetragonal. This transition can be compared with the antiferromagnetic transition in Cr and its alloys.^{15,16} The antiferromagnetic transition is believed to arise from the "nesting" characteristics of the bcc band structure and peaks at $\delta \approx 6.2$.¹⁷ The crystal structure of the V-Ru system is $B2$ so that the bcc Brillouin zone is already halved by the ordering of the V and Ru atoms. The transition from cubic to tetragonal does not further split the Brillouin zone but merely distorts it. Although the critical electron-atom ratio for the V-Ru system is somewhat larger than that for the antiferromagnetism in the Cr system, it may be that the transition in the V-Ru system is also related to the nesting property of the bcc structure. Thus the electronic band structure of the CsCl structure, where the nesting portions of the bcc band, the electron jack, and the hole octahedron have been remapped on top of one another, may be particularly sensitive to distortions. It would be of great interest to have a band-structure calculation of the $V_{0.50}Ru_{0.50}$ alloy assuming a completely ordered CsCl structure and to examine its stability against tetragonal distortions.

ACKNOWLEDGMENTS

The authors are grateful to F. Heiniger of Geneva for many helpful conversations, E. Corenzwit for discussion and preparation of the samples, A. Menth for the high temperature susceptibility measurements, and A. C. Gossard for performing the Knight-shift measurements. Discussions about the crystal structure at low temperature with M. Marezio and P. D. Dernier are very much appreciated. In particular, thanks are due to T. M. Rice for his valuable suggestions throughout this investigation.

*Present address: Physics Department, Cleveland State University, Cleveland, Ohio 44115.

¹F. Heiniger, E. Bucher, and J. Müller, *Physik Kondensierten Materie* **5**, 243 (1966).

²See M. Shimizu and A. Katsuki, *J. Phys. Soc. Japan* **19**, 1856 (1964), and references cited therein.

³E. Raub and W. Fritzsche, *Z. Metallk.* **54**, 21 (1963).

⁴R. Flükiger, F. Heiniger, and J. Müller, in *Proceedings of the Eleventh International Conference on Low Temperature Physics, St. Andrews, Scotland, 1968*, edited by J. F. Allen, D. M. Finlayson, and D. M. McCall (University of St. Andrews Printing Dept., St. Andrews, Scotland, 1969), p. 1017.

⁵J. Labbé and J. Friedel, *J. Phys. (Paris)* **27**, 153 (1966); **27**, 303 (1966).

⁶M. Bernasson, P. Descouts, P. Donzé, and A. Treyvaud, *J. Phys. Chem. Solids* **30**, 2453 (1969).

⁷M. Marezio, P. D. Dernier, and C. W. Chu (un-

published). It can also be a Martensitic transformation.

⁸D. B. McWhan and T. M. Rice, *Phys. Rev. Letters* **19**, 846 (1967), and references cited therein.

⁹W. C. Koehler, R. M. Moon, A. L. Trego, and A. R. Mackintosh, *Phys. Rev.* **151**, 405 (1966); A. L. Trego and A. R. Mackintosh, *Phys. Rev.* **166**, 495 (1968).

¹⁰F. J. Morin and J. P. Maita, *Phys. Rev.* **129**, 1115 (1963).

¹¹A. M. Clogston and V. Jaccarino, *Phys. Rev.* **121**, 1357 (1961).

¹²A. M. Clogston, A. C. Gossard, V. Jaccarino, and Y. Yafet, *Phys. Rev. Letters* **9**, 262 (1962).

¹³A. H. Wilson, *The Theory of Metals*, 2nd ed. (Cambridge U. P., London, 1953), p. 151.

¹⁴W. L. McMillan, *Phys. Rev.* **167**, 331 (1968).

¹⁵See A. W. Overhauser, *Phys. Rev.* **167**, 691 (1968), and references cited therein.

¹⁶W. M. Lomer, Proc. Phys. Soc. (London) 80, 489 (1962).

¹⁷F. Heiniger, Physik Kondensierten Materie 5, 285 (1966).

PHYSICAL REVIEW B

VOLUME 4, NUMBER 2

15 JULY 1971

Photoemission Studies of Platinum†

S. F. Lin, D. T. Pierce, and W. E. Spicer

Stanford Electronics Laboratories, Stanford University, Stanford, California 94305

(Received 25 March 1971)

Photoelectron energy-distribution curves of Pt at photon energies $6.8 \leq \hbar\omega \leq 11.6$ eV exhibit structure originating from initial states 3.6, 2.5, 1.5, and between 0.7 and 0.2 eV below E_F . A strong peak at -0.2 eV observed for $\hbar\omega < 9.1$ eV is joined by a second peak at -0.7 eV in the range $\hbar\omega = 9.1-9.7$ eV. Above 9.7 eV, the two peaks merge to a single rounded peak at -0.5 eV which grows stronger and sharper at higher photon energy. Good correspondence is found between structure in the energy-distribution curves and in a calculated band density of states. The results are discussed in terms of the direct and nondirect models of optical excitation and compared to similar results from Ni, Pd, and Rh.

I. INTRODUCTION

It is now well established that photoemission studies can give valuable information on the electronic structure of solids. In this paper we present data obtained from carefully prepared Pt samples. Earlier studies of Pt by Yu and Spicer¹ were hindered by poor vacuum conditions. In discussing the experimental results we compare the photoelectron energy-distribution curves (EDC) obtained in this work with the theoretically calculated valence-band density of states of Mueller *et al.*² Finally, as a link to the systematic study of transition metals, we compare the present work to results from Rh,³ Pd,⁴ and Ni.⁵

II. EXPERIMENTAL PROCEDURE

Photoelectron EDC's were obtained from Pt films electron-gun evaporated onto quartz substrates. The data presented in this paper are from a film approximately 600 Å thick. During the evaporation, the pressure changed from a base pressure of 10^{-10} to 1.5×10^{-8} Torr. A subsequent x-ray diffraction analysis displayed only peaks appropriate to an fcc crystal of (111) orientation.

The energy spectra of photoemitted electrons were measured with a three-electrode high-resolution energy analyzer.⁶ In this analyzer, a screen forms a field-free drift region around the emitter. The electrons are then retarded at the nearly spherical equipotential surfaces between the screen and the collector. The resolution error of the analyzer is estimated to be 2.8% of the electron kinetic energy.⁷ The EDC's were obtained by differentiating the current-retarding voltage curve by a previously described ac technique.^{8,9}

III. RESULTS

In Fig. 1 we compare the EDC's from this work to the EDC's obtained in the earlier work of Yu and Spicer. As can be seen, the position of structure is about the same in the two sets of curves.¹⁰ However, the high-energy or "leading" photoelectron peak is much stronger in our results than in the earlier work in which EDC's were obtained from films evaporated at 8×10^{-8} Torr. It is well established that the electron-electron scattering length becomes smaller as the electron energy increases. Thus, as the photon energy is increased, the electrons in the leading peak come from closer and closer to the metal surface. The fact that the leading peak in the curves of Yu and Spicer degrades with increasing photon energy may indicate that the band structure near the metal surface has been

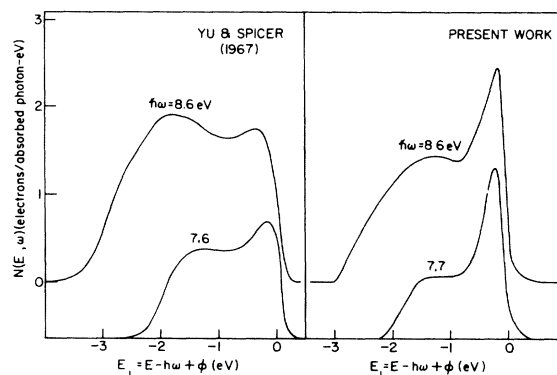


FIG. 1. Comparison of EDC's from the present work and the previous work of Yu and Spicer. Note the relatively fewer number of low-energy electrons in EDC's obtained from the better samples of the present work (normalized to the yield).